Asian Herpetological Research 2012, 3(1): 52–68
DOI: 10.3724/SP.J.1245.2012.00052

Phylogeography of the *Phrynocephalus vlangalii* Species Complex in the Upper Reaches of the Yellow River Inferred from mtDNA *ND4-tRNA^{LEU}* Segments

Xianguang GUO, Li LIU and Yuezhao WANG*

Chengdu Institute of Biology, *Chinese Academy of Sciences*, *Chengdu* 610041, *Sichuan*, *China*

Abstract The Ching Hai Toad-headed Agama (*Phrynocephalus vlangalii*) complex is a small toad-headed viviparous lizard that is endemic to the Qinghai-Tibetan Plateau. A fragment of mtDNA *ND4-tRNA^{LEU}* from 189 samples in 26 populations was used to infer the phylogeographic history of this species complex in the upper reaches of the Yellow River. Phylogenetic analyses revealed that *P. vlangalii* and another proposed species (*P. putjatia*) do not form a monophyletic mtDNA clade, which in contrast with a previous study, includes *P. theobaldi* and *P. forsythii*. Lineage diversification occurred in the Middle Pleistocene for *P. vlangali* (*ca.* 0.95 Ma) and in the Early Pleistocene for *P. putjatia* (*ca.* 1.78 Ma). The uplift of the A'nyemaqen Mountains and glaciations since the mid-late Pleistocene, especially during the Kunlun Glaciation, are considered to have promoted the allopartric divergence of *P. vlangalii*. The diversification of *P. putjatia* may be triggered by the tectonic movement in the Huangshui River valley during the C phase of Qingzang Movement. Subsequently, the glacial climate throughout the Pleistocene may have continued to impede the gene flow of *P. putjatia,* eventually resulting in the genetic divergence of *P. putjatia* in the allopatric regions. Demographic estimates revealed weak population expansion in one lineage of *P. vlangalii* (A2, the Qaidam Basin lineage) and one lineage of *P. putjatia* (B2, the north Qinghai Lake lineage) after approximately 42 000 years before present. However, constant population size through time was inferred for two lineages (A1 and B1), the source of Yellow River lineage of *P. vlangalii* and the southeast of Qinghai Lake lineage of *P. putjatia*, possibly due to stable populations persisting in areas unaffected by glacial advances. Our results also suggest: 1) at least four differentiated lineages of *P. vlangalii* complex may have evolved allopatrically in different regions during the Pleistocene glaciation events; 2) in support of several recent studies, *P. putjatia* is a valid species, having a more wide distribution than previously considered; and 3) a hypothesis referring to *P. v. hongyuanensis*, inhabiting in the source region of the Yellow River, being synonymous with *P. v. pylozwi* is supported.

Keywords agamid, diversification, historical demography, lineage, mtDNA, Pleistocene glaciations, Tibetan Plateau

1. Introduction

A fundamental premise of phylogeography is that geological events, climatic history, and environmental heterogeneity play an important role in population divergence and speciation (Avise, 2000). Phylogeographic analysis of DNA sequence data has been routinely used to determine species boundaries and speciation patterns, especially in the context of Quaternary and Holocene histories of regional biotas (Hewitt, 2001). The dramatic geological and climatic history and striking habitat diversity of the Qinghai-Tibetan Plateau (QTP), ranging from broad plantation surfaces, basins to mountain ranges, have made it a geographic focus of many phylogeographic studies (Jin *et al*., 2008; Qu *et al.*, 2010; Xu *et al*., 2010; Zhan *et al.*, 2011). As reviewed by Yang *et al*. (2009), the geomorphic and climatic changes on the plateau during the Quaternary have a remarkable influence on regional and adjacent biogeographic patterns.

The Quaternary glaciations in the QTP and the bordering mountains were the consequence of a combination between climate and local tectonic uplift.

* Corresponding author: Prof. Yuezhao WANG, from Chengdu Institute of Biology, Chinese Academy of Sciences, with his research focusing on taxonomy, phylogeny and biogeography of amphibians and reptiles.
E-mail: guoxg@cib.ac.cn (Xianguang GUO); arcib@cib.ac.cn (Yuezhao WANG)
Received: 3 November 2011 Accepted: 1 March 2012

In particular, the Kunlun-Huanghe and Gonghe tectonic uplifts have played very important roles in triggering glaciations in high Asia (Shi *et al.*, 2011; Zhao *et al*., 2011; Zhou *et al*., 2011). Although there is no evidence of a continuous ice sheet covering the whole Tibetan Plateau throughout the Quaternary glaciations (Li *et al.*, 1991; Zheng and Rutter, 1998; Zhou *et al.*, 2011), four discrete Pleistocene glaciations have been identified on the QTP and the bordering mountains. These four main Pleistocene glaciations are correlated with MIS 18–16, 12, 6 and 4–2 (Zhou *et al.*, 2011; and references therein). The most extensive glaciation in the plateau, Kunlun Glaciation, occurred during MIS 18–16 (0.78–0.62 Ma), which corresponds with the late Kunlun-Huanghe movement (0.7–1.1Ma, Cui *et al*., 1998). Several researchers suggested that current populations of some species originated from ancestors that recolonized this area from low-altitude refugia located at the plateau-edge during the Last Glacial Maximum (LGM, approximately 20 000 years ago). However, if no massive ice sheet developed on the QTP during the Pleistocene glaciations (Zhou *et al.*, 2011), it is highly likely that some cold-tolerant reptiles could have survived in ice-free areas of the plateau, even during glaciations.

The Yellow River originates from the Yuegouzonglie Basin on the north foot of the Bayan Har Mountains of the QTP, winding eastward and crossing the Loess Plateau and the Huang-Huai-Hai Plain into the Bohai Sea. Its formation and evolution is closely related to the uplift of the QTP during the Quaternary period (Jiang *et al.*, 2007; Li, 1993; Li *et al*., 1996; Liu and Sun, 2007; Zhang *et al.*, 2004). Li *et al.* (1996) discussed the geomorphological evolution of the Yellow River in the upper reaches and the relationship with QTP uplift, suggesting the initiation of the upper Yellow River was at 1.6 Ma near Lanzhou, and has experienced a strong incision since 0.15 Ma. Pan (1994) discussed the geomorphic evolution and development of the upper reaches of Yellow River in Guide Basin. He suggested that the Gonghe movement (0.15 Ma) made Guide Basin rise. The uplift and dry climate made Guide Basin lose the water link with the Qinghai Lake (also known as Koko Nor in Mongolian, and mTsho sngon po in Tibetan) in Late Pleistocene, and instigated the disappearance of the Gonghe-Guide-Qinghai palaeo-lake (Pan, 1994; Yuan *et al.*, 1990). Uplifting mountain ranges crossing the river course would have acted as boundaries for the eastern Qinghai palaeo-lake, near the Longyang gorges (Gonghe Basin exit), Shanba gorges (Guide Basin exit) or Jishi Gorges (Xunhua Basin exit). Madsen *et al.* (2008) proposed that Qinghai Lake began to form during the Middle or Late Pleistocene when the Riyue Shan uplift separated the Qinghai Basin from the Yellow River drainage system. The occurrence and development of the Quaternary glaciers in the upper reaches of Yellow River were also closely related to the amplitude and time of mountain uplifting and climatic conditions (Deng *et al.*, 2004; Zheng and Wang, 1996). Since the mid-Pleistocene epoch, three glaciations have occurred in the Bayun Har, Zarijia, Buqingshan and A'nyemaqen Mountains in the upper reaches of the Yellow River.

It has been long recognized that the phylogeny and taxonomy of the toad-headed agamas (*Phrynocephalus*) is very complex and controversial. Among the many controversies, the classification of the Ching Hai Toad-headed Agama (*Phrynocephalus vlangalii*) complex is perhaps one of the most confusing (Jin *et al.*, 2008). Historically more than ten names have been applied to *P. vlangalii* (Barabanov and Ananjeva, 2007). As for *P. putjatia*, Wang *et al.* (2002) considered it a valid species based on morphological and chromosomal differences, whereas most herpetologists regard it as a synonym of *P. vlangalii* (Zhao, 1999). Guo and Wang (2007) suggested that *P. putjatia* is a valid species, comprising populations from Guide, Qinghai Province and Tianzhu, Gansu Province; while *P. hongyuanensis* is not a valid species, synonymized instead with *P. vlangalii*. Subsequently, Jin *et al.* (2008) implied that *P. putjatia* is valid, and *P. v. hongyuanensis* is the synonym of *P. v. pylzowi* on the basis of mtDNA *ND2* fragment. Recently, Nobel *et al.* (2010) reconfirmed the validity of *P. putjatia* by using Bayesian model-based assignment tests of microsatellite DNA data. As for the distribution of *P. putjatia*, Bedriaga (1909) originally thought Guide County, Qinghai Province, China as the only known place. Until recently, *P. putjatia* was thought to occur in southeast of the Qinghai Lake (Jin, 2008). Accordingly, the distribution information for *P. putjatia* is still incomplete.

Although all mtDNA genes belong to a single linkage group and evolve as one locus, different mitochondrial genes may have different phylogenetic performance (Mueller, 2006; Zardoya and Meyer, 1996). In addition, individual mitochondrial genes might potentially produce misleading evolutionary inferences and hence might not constitute an adequate representation neither of the entire mitochondrial genome nor of the evolutionary history of the organisms from which they are derived. Accordingly, it is necessary to test the hypothesis of Jin *et al.* (2008) to clarify the evolutionary history of the *P. valangalii* species complex.

Here, we examine the phylogeography of the *P. vlangalii* species complex from the upper reaches of the Yellow River by conducting molecular phylogenetic, dating and population genetic analyses of mtDNA *ND4-tRNA*^{LEU}. We also include several haplotypes of *P. theobaldi* and *P. forsythii* (Pang *et al.*, 2003) as outgroup taxa to test the phylogenetic relationships among the viviparous group. This provides a framework for achieving the primary goal of testing relationships between physical events and/or climatic changes in the upper reaches of the Yellow River and genetic diversity among populations. The major goals of this study were to address the following questions: 1) What is the geographic structure of morphological and genetic variation among populations of the upper reaches of the Yellow River? 2) Did the uplifting of the A'nyemaqen Mountains or past glaciations promote the allopartric divergence of *P. vlangalii* and if so, when did it happen? 3) Was there a single refugium or multiple refugia in the upper reaches of the Yellow River and adjacent areas? In addition, we discuss the taxonomic implications of our preferred hypothesis relative to previous notions of viviparous *Phrynocephalus* species relationships (Guo and Wang, 2007; Jin *et al.*, 2008; Pang *et al.*, 2003).

2. Materials and Methods

2.1 Geographic sampling One hundred and seventy five *Phrynocephalus vlangalii* species complex specimens were collected from 24 sites across nearly the upper reaches of the Yellow River (Figure 1; Table 1). After being euthanized, liver or muscle tissues of individuals were dissected and preserved in 95% ethanol for genomic DNA extraction. Voucher specimens are held at the Chengdu Institute of Biology, Chinese Academy of Sciences. 14 published sequences (Table 1; Pang *et al.*, 2003) were also included in this study. Thus, a total of 189 individuals from 26 sites were included in this study. Voucher specimens and geographic localities corresponding to tissues used in this study are detailed in Table 1. *P. axillaris* and four other species were selected as outgroup taxa based on current understanding of the phylogenetic relationships among toad-headed lizards (Guo and Wang, 2007). The 16 sequences of the outgroup taxa were all retrieved from the GenBank.

2.2 DNA extraction, amplification and sequencing protocols Total genomic DNA was extracted from fixed liver or muscle tissue following the method of Aljanabi and Martinez (1997). A fragment of the

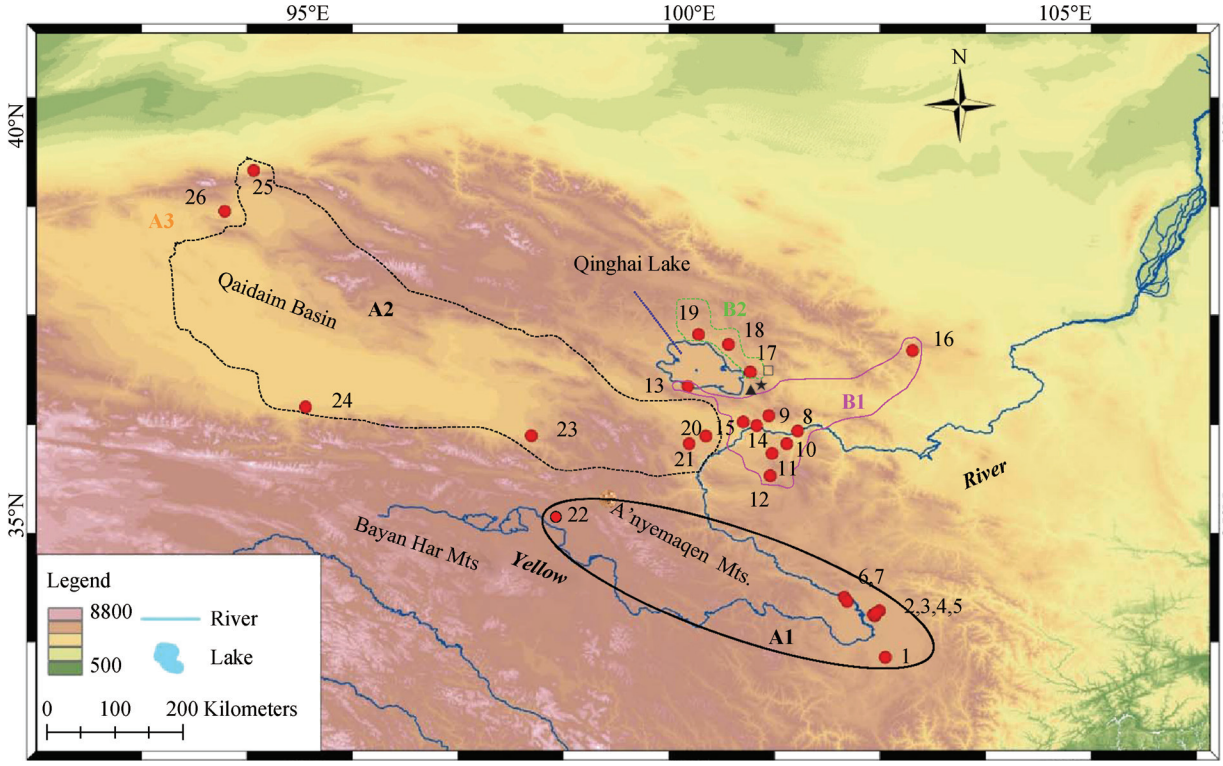

Figure 1 A map of the upper reaches of the Yellow River showing the sampling sites of *P. vlangalii* species complex (numbered red dots). Site names are listed in Table 1. Distributions of the main lineages identified in the phylogenetic trees are shown. ▲: Riyue Shan; ★: Xining City; □: Huzhu County.

mitochondrial gene encoding the fourth subunit of NADH dehydrogenase (plus downstream Serine, Histidine, and Leucine tRNAs; hereafter collectively referred to as *ND4-tRNA^{LEU}*) was amplified via PCR using the primers described in Arèvalo *et al*. (1994). Amplification was performed on the PTC-200 thermal cycler (Bio Rad) in a total volume of 50 μL containing 10 × reaction buffer (10 mM Tris-HCl, pH 8.3, 50 mM KCl, 1.5 mM $MgCl_2$), 0.1mM of each dNTP, 0.4 μM of each primer, 1.25 units rTaq polymerase (TaKaRa) and approximately 100 ng of template DNA. Thermal cycling was performed with an initial denaturation for 4 min at 94 °C followed by 35 cycles of 40 s at 94 °C, 40 s at 55 °C, 1 min at 72 °C with a final extension of 7 min at 72 °C. Negative controls were run for all amplifications. The amplified products were purified on a 0.8% agarose gel stained with ethidium bromide, using the DNA gel extraction kit (Omega Bio-Tek). The purified products were sequenced directly by Invitrogen Trading (Shanghai) Co., Ltd., using the same primers as PCR. The sequences were deposited in GenBank with accession numbers EU294028–EU294095, JF736517–JF736619.

2.3 Sequence alignment and analyses A total of 205 sequences were first aligned using ClustalX 1.83 (Thompson *et al.*, 1997) with default gap penalties. These alignments were rechecked based on inferred amino acid sequence homology (protein coding region) and secondary structure models (for tRNA regions; Macey and Verma, 1997) using MEGA v.4 (Tamura *et al*., 2007). This final alignment consisted of a total of 703 aligned positions (bases), three of which were inferred as gaps (relative to outgroup sequences) occurring in the loop structures of tRNAs in *P. vlangalii*. The data matrices are available from the first author.

Compositional heterogeneity was evaluated using Chi-square (χ^2) tests implemented in PAUP* 4.0b10 (Swofford, 2003) and assessed using the software SeqVis v.1.5 (Ho *et al*., 2006) to visualize base composition and to conduct matched-pairs tests of symmetry of base substitution (Ababneh *et al*., 2006). Evidence of evolution under conditions more complex than that assumed by commonly applied models (i. e., stationary, reversible and homogeneous conditions) was inferred if the scatter of dots in the tetrahedral plots was widely dispersed and if a proportion X of the matched-pairs tests of symmetry rejected symmetry with P-values less than or equal to X. This procedure is consistent with that advocated by Jermiin *et al*. (2008, 2009). If the matched-pairs tests yield a larger than expected proportion of probabilities ≤ 0.05 (i. e., with > 5% of the tests producing probabilities ≤ 0.05), then the conclusion is that the sequences have not evolved under stationary, reversible and homogeneous conditions.

2.4 Phylogenetic analyses Phylogenetic hypotheses were generated with *ND4-tRNA^{LEU}* segments using two commonly applied phylogenetic methods: heuristic searches using equally weighted maximum parsimony (MP) analyses performed with the program PAUP* and Bayesian inference (BI) with the program MrBayes v.3.2 (Ronquist and Huelsenbeck, 2003). In both MP and BI analyses, each haplotype was treated as a taxon and each nucleotide was treated as a character, and gaps were treated as missing data.

For heuristic searches under parsimony, invariant characters were removed from the dataset, and all remaining characters were treated as equally weighted. Each search involved ten random addition replicates, one tree held at each step, TBR branch swapping, steepest descent on, and a maximum of 100 000 saved trees; all other search settings were left at default values. Non-parametric bootstrapping was used to generate phylogeny confidence values (Felsenstein, 1985), with 1 000 pseudoreplicates using a heuristic tree search for each pseudoreplicate. These are presented as a majority consensus tree where branches with support lower than 50% are collapsed. *P. axillaris* was used to root the trees based on a recent publication (Guo and Wang, 2007). Because intraspecific gene evolution cannot always be represented by a bifurcating tree, haplotype networks may more effectively portray the relationships among haplotypes within species [reviewed by Posada and Crandal (2001)]. Therefore, we constructed unrooted parsimony networks of haplotypes for *P. vlangalii* species complex using TCS v.1.21 (Clement *et al*., 2000).

The appropriate models for the BI analyses were selected using Akaike Information Criterion (AIC; Akaike, 1974) in the program MrModeltest 2.3 (Nylander, 2008) with each starting tree obtained using the neighbor-joining algorithm in PAUP*. Sites in the *ND4-tRNA^{LEU}* alignment were partitioned *a priori* into classes based on general evolutionary constraints, and Bayes factors were calculated to determine the optimal partitioning scheme (Brandley *et al.*, 2005). Two partitioning schemes were assessed: one partition (one model for all sites), four partitions (1st codons, 2nd codons, 3rd codons, all other tRNA sites). The marginal likelihood of each partitioning scheme was approximated using the stepping-stone approach (Fan *et al*., 2011; Xie *et al*., 2011) implemented in Phycas (Lewis *et al*., 2008). Bayes factors strongly favored four partitions over one partitioning scheme (2ln

Bayes factor = 242.282). Models chosen were as follows: GTR + G + I (1st codon position); HKY (2nd codon position); GTR (3rd codon position); HKY + I (tRNAs positions).

We estimated posterior probability distributions by allowing four incrementally heated Markov chains (default heating values) to proceed for 2×10^7 generations, with samples taken every 1 000 generations. Analyses were repeated beginning with different starting trees to ensure that our analyses were not restricted from the global optimum (Huelsenbeck *et al*., 2002). MCMC convergence was explored by examining the potential scale reduction factor (PSRF; Gelman and Rubin, 1992) convergence diagnostics for all parameters in the model (provided by the *sump* and *sumt* commands) and graphically using the program Tracer v.1.5 (Rambaut and Drummond, 2009). The first four million generations, before this chain reached apparent stationarity, were discarded, and the remaining samples from the independent runs were pooled to obtain the final approximation of the posterior distribution of trees. To yield a single hypothesis of phylogeny, the posterior distribution was summarized as a 50% majority-rule consensus.

2.5 Bayesian hypothesis testing Bayes factors were used to compare the preferred Bayesian tree topology (see below) to Bayesian trees with constraint. This method differs from traditional hypothesis testing because it does not offer a criterion for absolute rejection of a null hypothesis but instead an evaluation of the evidence in favor of the null hypothesis (Kass and Raftery, 1995). The phylogeny inferred from the *ND4-tRNA^{LEU}* data set was constrained to alternative hypotheses. Constraint analyses were conducted in MrBayes v.3.2 using the command *prset topologypr = constraint*. All analyses consisted of two simultaneous runs each with an abbreviated three MCMC chains run for 20 million generations. The Bayes factor was determined by calculating the marginal likelihood for both unconstrained and constraint analyses using TRACER v.1.5 (Rambaut and Drummond, 2009). The difference in these ln-transformed marginal likelihoods was compared to the table provided by Raftery (1996). Based on the table, we consider a 2ln Bayes factor ≥ 10 as significant evidence for a hypothesis (Kass and Raftery, 1995).

2.6 Divergence-time estimation BEAST v.1.6.1 (Drummond and Rambaut, 2007) was used to estimate divergence time of lineages under a Bayesian statistical framework. As no direct fossil records of *Phrynocephalus* have so far been detected in Chinese fossil layers (Zerova and Chkhikvadze, 1984), we used the average nucleotide substitution rate of *ND4*, 1.17% (with 95% credibility interval 0.85%–1.81%) per site per million years (estimated from the data of Guo and Wang, 2007) among lineages, to date lineage divergences based on the uncorrelated lognormal relaxed clock model and a Yule process tree prior (Drummond *et al.*, 2006). Analyses were performed using an HKY+G substitution model (best-fit model based on AIC in MrModeltest). The MCMC chain was run for 2×10^7 generations, and it was sampled every 1 000 generations with the first 10% discarded as burn-in. Convergence of the MCMC chain to stationary distribution and adequate sampling were checked in TRACER. We performed the analysis three times to confirm the stability and convergence of the MCMC chains. The results were found to be satisfactory and samples from the multiple runs were combined.

2.7 Demographic analyses Genetic diversity estimates were calculated for separate lineage of the *P. vlangalii* species complex using DnaSP v.5.0 (Librado and Rozas, 2009). These include haplotype diversity (h) and nucleotide diversity (π). Mismatch distributions were calculated for each diagnosed population lineage to infer changes in population size with ARLEQUIN v.3.5 (Excoffier and Lischer, 2010). To compare the observed data with the expected data under the sudden expansion model, we conducted goodness-of-fit tests based on the sum of squared deviations (SSD) and Harpending's raggedness index (r_g) (Harpending, 1994) using 10 000 parametric bootstrap replicates. Although the raggedness index (r_g) is often used to assess significance of mismatch plots, multi-modal distributions that fit sudden-expansion models indicate structuring within populations or populations that are stable or shrinking (Rogers and Harpening, 1992). Therefore we do not consider the good fit of sudden-expansion models to unimodal mismatch distributions strong evidence of population expansion. Given that tests based on the mismatch distribution have little power against population growth, Tajima's D (1989), Fu's F_S (Fu, 1997) and *R2* statistic (Ramos-Onsins and Rozas, 2002) were calculated in DnaSP as additional assessments of possible population expansion. Significance of D, F_S and *R2* values was determined in DnaSP using 1 000 simulated samples to produce an expected distribution under selective neutrality and population equilibrium. The cut-off level for statistical significance was 0.05. For Fu's F_S, significance at the 0.05 level was indicated when P values were < 0.02 (Excoffier and Lischer, 2010). If significant statistic-values of Fu's *Fs*, Tajima's D and *R2* are obtained, a population

Table 1 The sampling locations, number of specimens (n), and voucher number for the samples of *P. vlangalii* complex used in this study.

Site label	Location code	Sampling location	n	Coordinates	Voucher numbers*
1	HY	Hongyuan	9	N33.17649 E102.62830	DLW200607001–2, DL050002–5, 2LDW001, *0714*, *0541*
2	XMa	Xiaman A	17	N33.70605 E102.48526	DLW200607007–9, DLW200607011–15, DLW200607017–23, *Xm276, Xm277*
3	XMb	Xiaman B	9	N33.77507 E102.54921	DLW200607024–26, DLW200607029–34
4	XMc	Xiaman C	13	N33.72512 E102.46995	DLW200607035–40, DLW200607042–46, DLW200607048, DLW200607050
5	XMd	Xiaman D	8	N33.74796 E102.50430	DL050011–15, DL050017–18, DL050020
6	MQa	Maqu A	8	N33.95074 E102.08892	DLW200607052, DLW200607054–55, DLW200607057–58, DLW200607060–62
7	MQb	Maqu B	8	N33.89865 E102.12673	DLW200607064–70, DLW200607072
8	GDA	Guide A	11	N36.08161 E101.46884	DLW200607074–76,78–83; *0771*,*0772*
9	GDB	Guide B	8	N36.27295 E101.08978	DLW200607084–87,103–106
10	GDC	Guide C	7	N35.91614 E101.32405	2WDL0508028-30, 32, 33, 35, 38
11	GNA	Guinan A	5	N35.79170 E101.13223	2WDL0508044–48
12	GNB	Guinan B	2	N35.50655 E101.10550	2WDL0508059, 60
13	HM	Heimahe	11	N36.65030 E100.01867	DLW200607138–148
14	GHA	Gonghe A	5	N36.15008 E100.92765	DLW200607109–113
15	GHB	Gonghe B	7	N36.19800 E100.74776	DLW200607114–120
16	TZ	Tianzhu	8	N37.11158 E102.99005	WGL070602–08; *0709*, *0769*
17	HYA	Haiyan A	8	N36.83891 E100.84207	DLW200607123–128,135
18	HYB	Haiyan B	6	N37.18976 E100.55337	DLW200607155–160
19	GC	Gangcha	6	N37.31397 E100.15899	DLW200607149–154
20	XHA	Xinghai A	4	N36.01592 E100.25779	2WDL0508052, 53, 55, 56
21	XHB	Xinghai B	6	N35.91789 E100.03450	GXG07080071,74-78
22	MD	Maduo	8	N35.20496 E98.97128	GP0708073–80
23	DL	Dulan	6	N36.01934 E97.95179	*0792*, *0793*, *0796*, *0797*; GP0708159, 162
24	GM	Golmud	6	N36.38700 E94.96739	GP0708255, 257, 258; *Rdq1–3*
25	AKS	Akesai	1	N39.41941 E94.28142	*740*
26	SGH	Suganhu	2	N38.89919 E93.89908	*0970*, *0972*

*: The DNA data of the samples in italic were retrieved from GenBank.

expansion model cannot be rejected.

To further evaluate the signature of population fluctuations through time, we constructed Bayesian skyline plots (BSP; Drummond *et al.* 2005) implemented in BEAST. As above, the appropriate model of nucleotide substitution for each lineage was determined using MrModeltest. Separate analyses were performed for each lineage, with the exception of A3. Multiple analyses were performed to test for convergence, with each data set run twice for 2×10^7 iterations and sampled every 1 000 iterations with the first 10% initial samples discarded as burn-in under a strict clock, stepwise skyline model and uniform priors. Results from replicate runs were pooled using LogCombiner and skyline plots generated using TRACER. To convert estimates into units of time, we used mean substitution rate of 1.5% per site per million years as a heuristic, which was obtained from the BEAST analysis (See above).

3. Results

3.1 Base composition and nucleotide substitution patterns

The sequence comprised 703 aligned sites, including 578 bp of partial *ND4*, 125 bp of *tRNAs* for all samples of the *P. vlangalii* complex. Alignment was unambiguous and 3 indels were inferred among *P. vlangalii* species complex. No premature stop codons were observed in *ND4*, indicating that the obtained sequences were mitochondrial in origin and not nuclear pseudocopies. A total of 39 haplotypes were revealed within the 189 individuals by 110 polymorphic sites containing 4 singleton variable sites. No haplotypes were geographically widespread. Haplotypes shared across populations were just found in some geographically proximate localities and the rest 32 ones were private for each locality (Table 2).The majority of variables of the 703 bp were from *ND4* (85.5%), with the third codon position (53.6%). The first (24.5%) and second (7.3%) variable positions were relatively low. The average proportions of base composition were $T = 0.252$, $C = 0.261$, $A = 0.361$, and $G = 0.126$. Nucleotide composition showed an anti-G bias and A+T-richness (61.3%), which is a characteristic of the mitochondrial genome.

A base stationarity test shows insignificant differences

Table 2 The distribution of the haplotypes (haplotype 1–39) in the population of *P. vlangalii* complex analyzed.

Population*	H	H	H	H	H	**H**	H	H	H	H	**H**	H	H	H	H	H	H	H	H	H	**H**	H	H	**H**	H	H	H	**H**	H	H	H	H	H	H	H	Total
	1	2	3	4	5	**6**	7	8	9	10	**11**	12	13	14	15	16	17	18	19	20	**21**	**22**	**23**	24	25	26	27	**28**	29	30	31	**32**	33	34	35	36	37	38	39	
GD	4	7																																						11
GDB			2	1	1	**4**																																		8
GDC							7																																	7
GNA																2	2	1																						5
GNB																			1	1																				2
HM						**11**																																		11
GHA								5																																5
GHB									7																															7
TZ																														6	2									8
HYA										4	**2**	1	1																											8
HYB											**3**			2	1																									6
GC											**6**																													6
XHA																					**4**																			4
XHB																					**6**																			6
HY																						**7**	**2**																	9
XMa																							**3**	11	3															17
XMb																							**9**																	9
XMc																							**4**	6		1	1	**1**												13
XMd																						**2**	**4**	2																8
MQa																													8											8
MQb																												**8**												8
MD																																				6	2			8
DL																																**3**	1	2						6
GM																																**5**			1					6
SGH																																						2		2
AKS																																							1	1
n	4	7	2	1	1	15	7	5	7	4	11	1	1	2	1	2	2	1	1	1	10	9	22	19	3	1	1	9	8	6	2	8	1	2	1	6	2	2	1	189

*: n, the number of individuals for each haplotype shaped. Haplotypes shared are in bold.

among all taxa (including 39 haplotypes and 16 outgroup taxa sequences) in base composition bias in the *ND4* data (χ^2 = 55.64, *df* = 162, *P* = 1.00). However, base composition at the third position exhibited significant heterogeneity: first position, χ^2 = 15.99, *df* = 162, *P* = 1.00; second position, χ^2 = 2.97, *df* = 162, *P* = 1.00; third position, χ^2 = 209.26, df = 162, *P* = 0.007; and tRNAs, χ^2 = 8.89, *df* = 162, *P* = 1.00. When all the sites are considered equal (i. e., all the sites placed in the same bin) and the tetrahedron is allowed to rotate, the 55 points are scattered tightly in an area where the proportion of *A* and *C* are > 25% (Appendix 1A). The points are clearly spread within a confined area, implying that there may be more compositional heterogeneity in these data than the initial analysis suggested. To address this issue, we binned the nucleotides according to the structural information. The distributions of points differ for the first, second, and third codon sites, with first codon sites displaying a small amount of scatter (Appendix 1B), second codon sites displaying hardly any scatter (Appendix 1C), and third codon sites displaying a lot of scatter (Appendix 1D). The tRNAs sites also displayed a small amount of scatter (Appendix 1E). Rotating the four tetrahedral plots shows that the centroids differ for the codon sites and tRNAs sites, thus suggesting that it would be necessary to apply four Markov models to these data to analyze them appropriately within a phylogenetic context. To corroborate whether this is the case, the matched-pairs test of symmetry is used in conjunction with *ND4-tRNA*^{LEU}, 1st, 2nd 3rd codon sites and tRNAs sites of the alignment. Table 3 summarizes the distribution of *P*-values for *ND4-tRNA*^{LEU}, 1st, 2nd and 3rd codon sites and tRNAs sites. Of the 1.081 pairwise tests conducted: 1) seventeen tests (0.0157) for 1st codon site were found to produce a probability ≤ 0.05, implying first codon site is consistent with evolution under stationary, reversible, and homogeneous conditions; 2) seven tests (0.0065) for 2nd codon site were found to produce a probability ≤ 0.05; 3) two hundred and thirty five (235) tests (0.2714) for third codon site were found to produce a probability ≤ 0.05, implying 3rd codon site is inconsistent with evolution under stationary, reversible, and homogeneous conditions. Given these results, a sensible approach to analyze these data phylogenetically would be to apply a time-reversible Markov model to the 1st codon sites, another such model to the 2nd codon sites, and a more general Markov model to the 3rd codon sites.

3.2 Phylogenetic analyses The heuristic search of the *ND4-tRNA*^{LEU} matrix resulted in 228 871 equally parsimonious trees of 423 steps, with moderate CI (0.5816) and high RI (0.9052). These are presented as a majority-rule consensus tree where branches with bootstrap support lower than 50% are collapsed (Appendix 2). For the BI analyses, the 50% majority consensus tree is shown in Figure 2. The average PSRF was 1.000, implying convergence of runs. The MP and Bayesian trees differed in bootstrap support values, but not in the compositions of the major lineages. The parsimony bootstrap support was also marked on the branches that receive such support in the Bayesian tree (Figure 2). The two analyses strongly support monophyly of the viviparous group with high support values (BP = 100%; PP = 1.0). Haplotypes corresponding to *P. theobaldi* and *P. forsythia* were found to be nested within the main *Phrynocephalus vlangalii* complex clade. Clade B (*P. putjatia*) is the sister taxon to the remaining viviparous species. Accordingly, *P. putjatia* and the other putative subspecies of *P. vlangalii* together did not form a single monophyletic clade. These comprise two distinct clades (A and B), being further subdivided into smaller

Table 3 Matched-pairs tests for stationarity of base composition. Using 1 081 tests for symmetry of base substitution, the number and proportion of tests rejecting the hypothesis of symmetry at the threshold level in column 1 are listed separately for tests using all *ND4-tRNA*^{LEU} base sites, 1st, 2nd and 3rd positions as well as tRNAs sites only. Because the proportions of statistically asymmetrical result of 3rd codon positions exceeds the threshold levels, we judge the 3rd codon positions primarily inconsistent with a model of base compositional stationarity.

Threshold*	*ND4-tRNA*^{LEU}		1st codon positions		2nd codon positions		3rd codon positions		tRNAs	
	Number	Proportion	Number	Proportion	Number	Proportion	Number	Proportion	Number	Proportion
0.05	229	0.2118	17	0.0157	7	0.0065	235	0.2714	0	0
0.01	54	0.0499	0	0	0	0	65	0.0601	0	0
0.005	32	0.0296	0	0	0	0	35	0.0324	0	0
0.001	5	0.0046	0	0	0	0	4	0.0037	0	0
0.0005	1	0.0009	0	0	0	0	0	0	0	0
0.0001	1	0.0009	0	0	0	0	0	0	0	0
0.00005	1	0.0009	0	0	0	0	0	0	0	0

*: The smallest *P* value for *ND4-tRNA*^{LEU} is 0.0000, for the 1st codon positions is 0.0455, for the 2nd codon positions is 0.0237, for the 3rd codon positions is 0.0005, and for tRNAs positions is 0.0719.

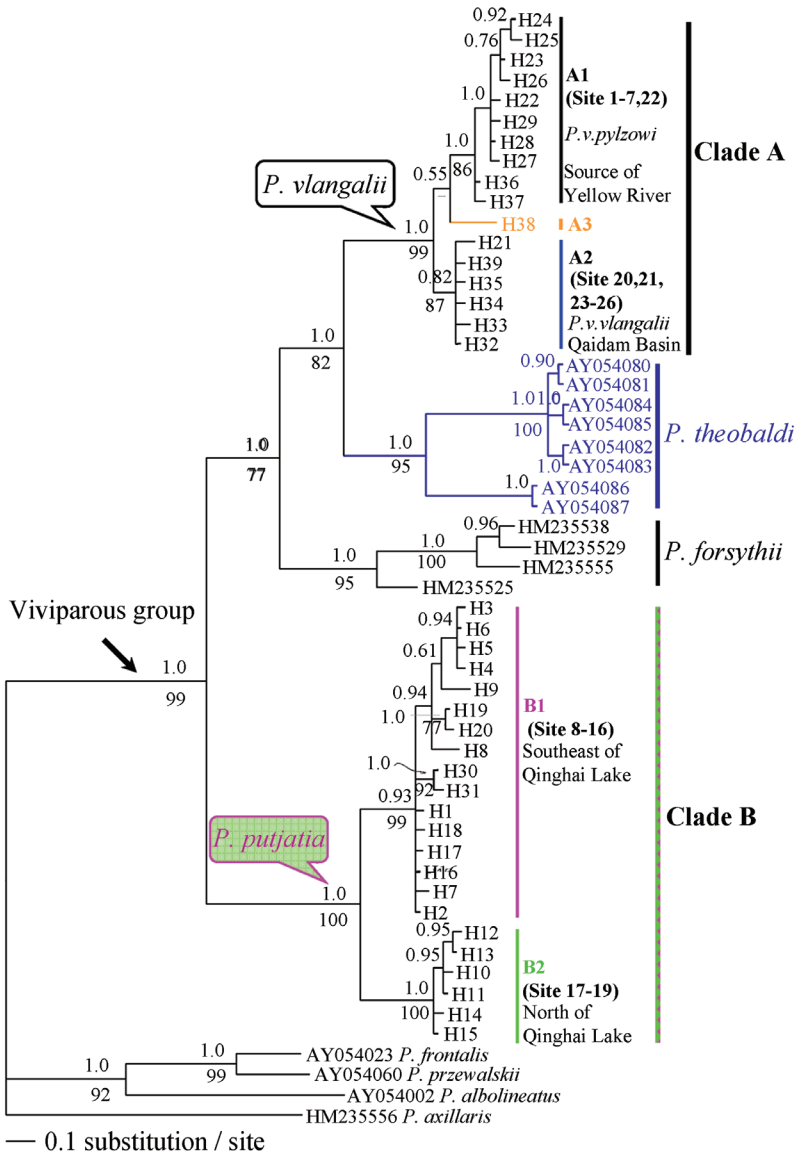

Figure 2 *ND4-tRNA*^{LEU} majority-rule consensus tree inferred from partitioned Bayesian inference by using MrBayes v.3.2, associations with less than 0.5 posterior probability were collapsed. Bayesian posterior probabilities, maximum parsimony bootstrap values are shown.

subclades: (i) source of Yellow River populations (A1), Qaidam Basin populations (A2), and Suganhu population (A3); and (ii) populations inhabiting the Qinghai Lake basin, corresponding to *P. putjatia* (B), which are subdivided into populations found to the north (B1) and southeast (B2) of the lake. However, the relationships between A1, A2 and A3 are ambiguous.

To get additional insight into the relationships among the *P. vlangalii* complex, we analyzed our data set, using the coalescent-based statistical parsimony network approach. The five unconnected networks revealed by TCS are given in Figure 3. These generally correspond to the five described phylogenetic lineages. The two networks corresponding to lineages A1 and A2 are connected by H36 and H32, with eight mutation steps. There are several unobserved intermediate haplotypes, representing unsampled or extinct haplotypes. The haplotype network of lineage B1 showed a star-like clustering. H2 (from GuideA, site 8) seemed to be a central haplotype, with six other haplotypes connected by 1–3 mutation steps.

3.3 Bayesian hypothesis testing Bayes factor analysis reflects our primary interests of evaluating the alternative hypotheses of interrelationships of viviparous species of *Phrynocephalus*. As mentioned above, analyses of the *ND4-tRNA*^{LEU} data yielded a non-monophyletic *P. vlangalii* complex. Bayes factor analyses of the *ND4-tRNA*^{LEU} data were conducted to compare topologies with constraints to the Bayesian tree topology. There was very

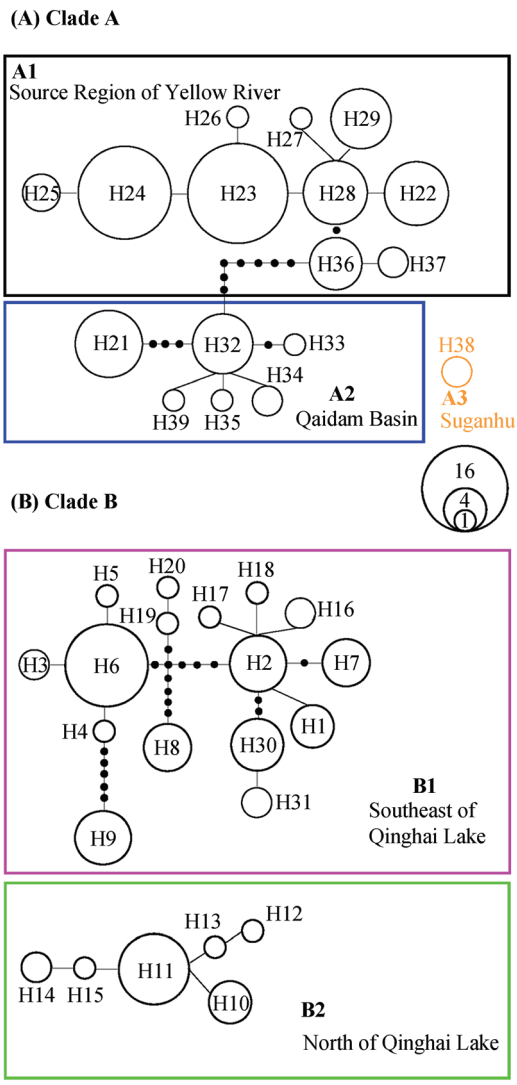

Figure 3 Statistical parsimony network showing genetic relationships and distance among 39 haplotypes of *P. vlangalii* species complex from different populations. In the network, hollow circles indicate sampled haplotypes, and small solid circles indicate unsampled or extinct haplotypes. Each mutation step is shown as either a short or longer line connecting neighboring haplotypes (including observed and unobserved one). The size of the hollow circles roughly represents the numbers of samples carrying the haplotype, with the scale given beside the network.

strong evidence against the constrained monophyly of *P. vlangalii* complex ($\text{Ln}L_{\text{unconstrained}}$ = –3053.657, $\text{Ln}L_{\text{constrained}}$ = –3067.845; 2ln Bayes factor = 28.376, > 10). Thus, the monophyly of *P. vlangalii* complex is significantly rejected.

3.4 Divergence times Bayesian estimates of divergence times are given for the major nodes in Figure 4. Dates ranged from 4.84 Ma (95% highest posterior density interval-HPD of 2.97–8.03 Ma) for the initial divergence of viviparous *phryncoepahlus* group to 0.95 Ma (95% HPD: 0.48–1.71 Ma) for cladogenesis within clade A and 0.29 Ma (95% HPD: 0.09–0.65 Ma) for divergence within lineage B2.

3.5 Historical demography Haplotype diversity (h) and nucleotide diversity (π) within each lineage were listed in Table 4. Genetic diversity of lineage B2 was lower than those of other lineages. Among four lineages, the highest haplotype diversity and nucleotide diversity was from lineage B1 (h = 0.892, π = 0.0087). Graphs of the mismatch distribution (Figure 5) indicate a significant unimodal distribution suggesting expansive population growth for all lineages, although the lineage A2 appears slightly bimodal. Confirming the mismatch distribution, tests of the observed SSD and r_g statistics in these lineages were small and not statistically significant at the 0.05 level (Table 4), indicating that the sudden expansion model could not be rejected for any of the lineages. However, this pattern was not detected by Tajima's D, Fu's *Fs* and *R2* statistics, with non-significant statistic values for all lineages (Table 4). This further indicated that all lineages were evolving in a neutral manner, i.e., in mutation-drift equilibrium. This incongruence can be explained by the fact that tests based on the mismatch distribution have little power against population growth (Ramos-Onsins and Rozas, 2002). It is noted that the number of segregating sites has a substantial effect on the power of Tajima's D, Fu's *Fs* and *R2* tests, which has been shown to have

Table 4 Summary of genetic diversity indices, mismatch distribution analysis and neutrality tests. Number of individuals (N), haplotypes (K) and segregating sites (S) , haplotype diversity (h), nucleotide diversity (π), sum of squared deviations (SSD), Harpending's raggedness index (r_g), Tajima's D, Fu's *Fs* and *R2* tests are indicated.

Lineage	*N*	*K*	*S*	*h*	π	*rg*	*SSD*	*R2* statistic	Tajima's D	Fu's *Fs*
A1	80	10	9	0.8351	0.0026	0.03469	0.00153	0.1013	0.00855	-1.513
A2	23	6	8	0.7075	0.00293	0.16532	0.07852	0.1224	-0.1679	0.7109
B1	64	15	27	0.8924	0.00872	0.03623*	0.01936	0.1128	0.228	0.6273
B2	20	6	5	0.6737	0.00155	0.04654	0.00037	0.1076	-0.7059	-2.016
A1+A2+A3	105	17	31	0.8908	0.0083	0.01483	0.02076	0.0931	-0.05095	0.6983
B1+B2	84	21	49	0.92	0.01934	0.0303	0.04242	0.1379	1.2424	3.2063

The results of the observed mismatch distribution against a sudden expansion distribution are reported as the Harpending (1994) raggedness r_g statistic and the sum of squared deviations (SSD). No mismatch distribution statistics were significantly different from the sudden expansion model, with exception to r_g for lineage B1. However, no neutrality tests statistics were significant. All values for each of these tests are non-significant above the threshold P = 0.05 except *.

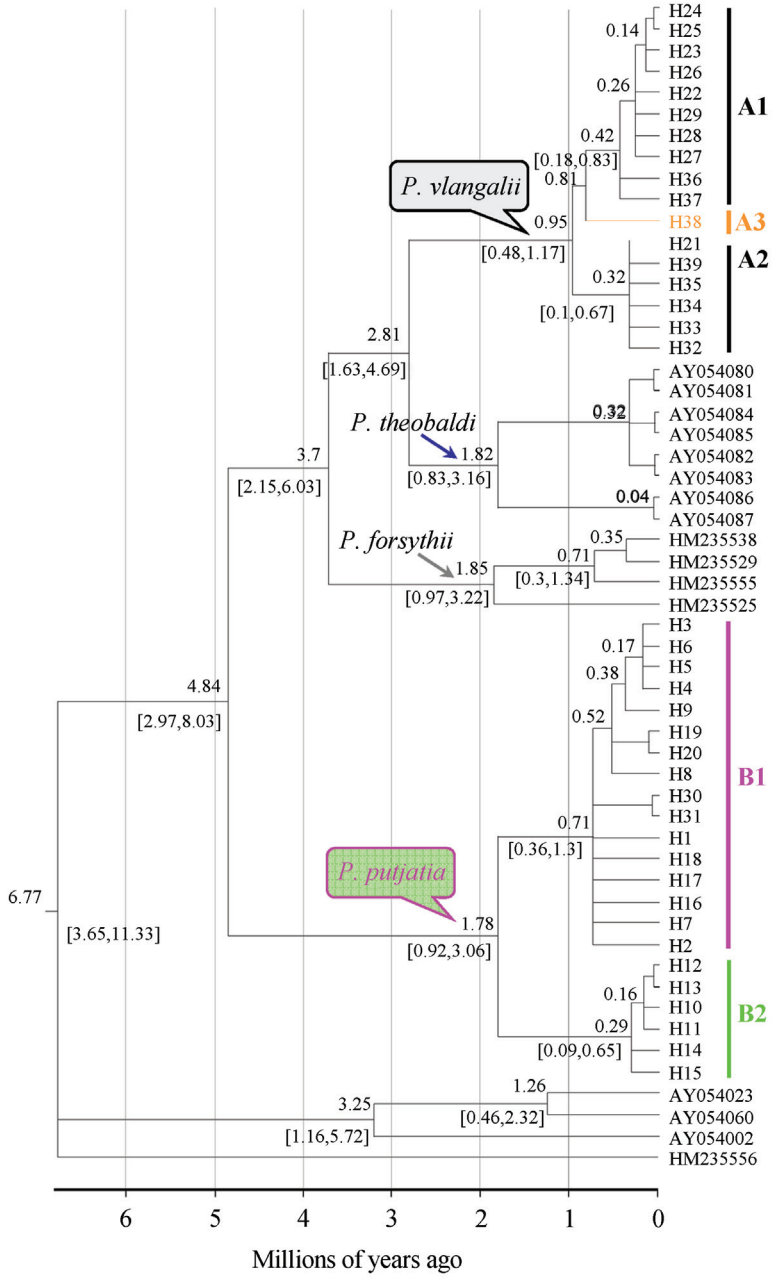

Figure 4 Chronogram showing results from the uncorrelated lognormal Bayesian relaxed clock in BEAST v.1.6.1. Numbers and the numbers in brackets below the nodes are the posterior mean ages and 95% HPD, respectively.

more power against population growth than tests based on the mismatch distribution such as r_g. The number of segregating sites (*S*) ranged between 5 and 14 for the four lineages tested, which is below the point at which these three tests lose power. Low number of segregating sites also results in similar mismatch distributions for both constant populations and expanding populations (Ramos-Onsins and Rozas, 2002). For this reason, coalescent methods such as BSP, which take genealogy into account, may provide a better estimate of demographic history given these data.

The coalescence-based Bayesian demographic analyses depicted the detailed fluctuations of effective population size for the four lineages (Figure 6). Median estimates from the BSP revealed weak population expansion in one lineage of *P. vlangalii* (lineage A2, the Qaidam Basin lineage) and one lineage of *P. putjatia* (lineage B2, the north of Qinghai Lake lineage). It should be noted that error around these estimates of *Ne* through time must be considered and this reduces certainty in

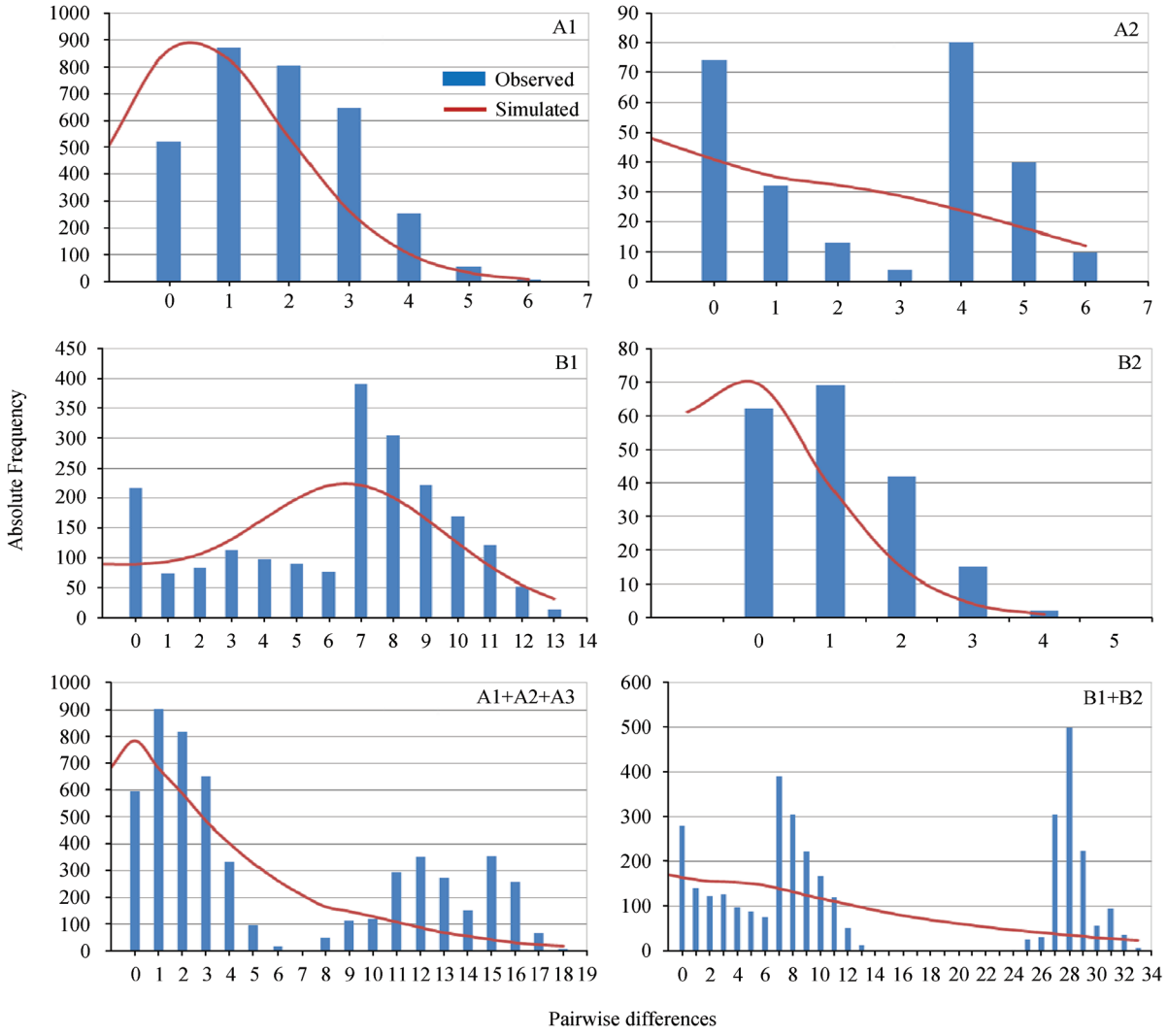

Figure 5 Mismatch distribution for observed frequencies of each lineage of *P. vlangalii* species complex compared to the simulated frequencies for sudden (stepwise) population expansion.

demographic trajectories for all lineages. Lineages A2 and B2 appear to have experienced a long period of relatively constant population size, followed by weak expansion after approximately 42 000 years before present. The population growth rate of A2 was higher than that of B2. Compared with A2 and B2, lineages A1 (the source of Yellow River lineage) and B1 (the southeast of Qinghai Lake lineage) appear to have remained stable over the last 200 000 and 650 000 years, respectively.

4. Discussion

4.1 Phylogenetic relationships of *Phrynocephalus vlangalii* species complex Monophyly of the viviparous group was recovered from *ND4-tRNA*^{LEU} data, which is consistent with the previous hypothesis (Guo and Wang, 2007; Pang *et al*., 2003). To date, however, the intra-relationship of viviparous species is still equivocal. Guo and Wang (2007) proposed that the *P. vlangalii* complex is paraphyletic with *P. theobaldi* /*P. zetangensis* on the basis of analyzing 2065 bp mtDNA data (*12S, 16S, cyt b, ND4-tRNA*^{LEU}). Later, Jin *et al.* (2008), on the basis of 609 bp mtDNA *ND2-tRNA* ^{ALA} fragments, revealed that *P. vlangalii* and two other species (*P. erythrurus* and *P. putjatia*) together form a clade which excludes *P. theobaldi* and *P. zetangensis*. The main discrepancy of the two hypotheses lies in the different phylogenetic placement of *P. putjatia*. In support of Guo and Wang (2007), our results corroborate the non-monophyly of *P. vlangalii* species complex. In contrast with Guo and Wang

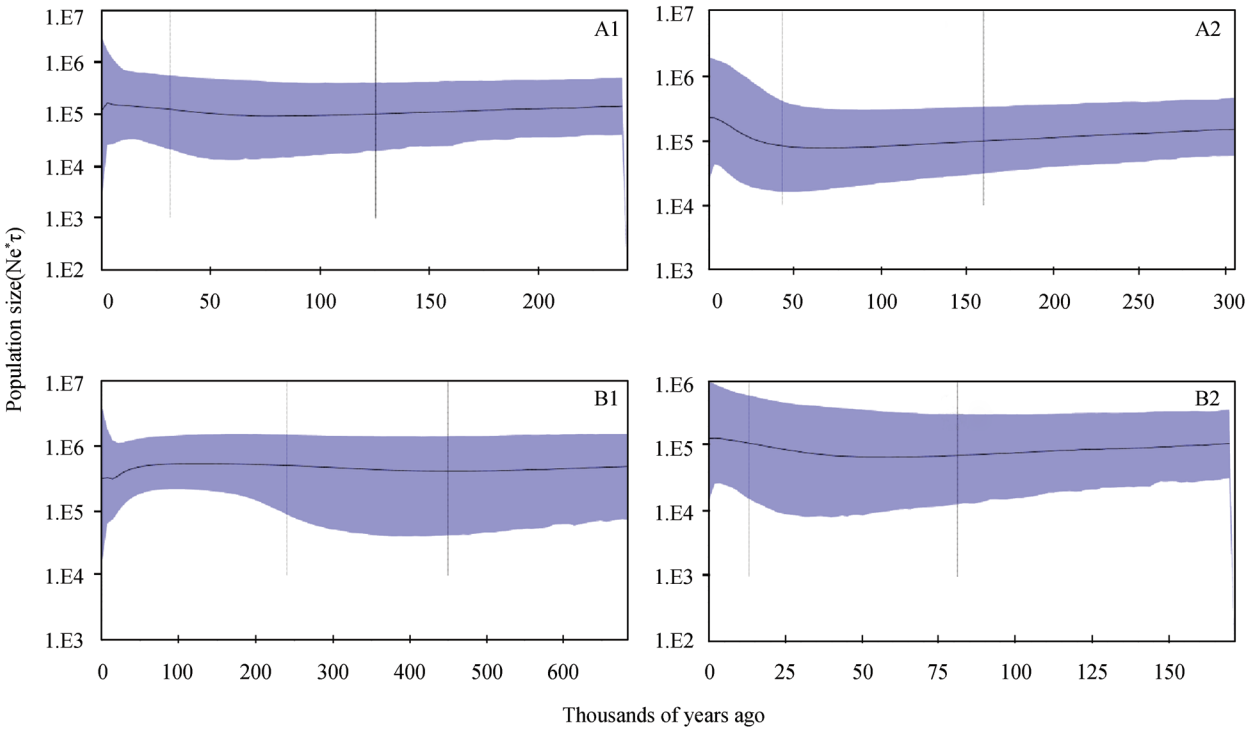

Figure 6 Bayesian skyline plots based on a mean mutation rate of 1.5×10^{-8} per site per year. The x-axis is in units of thousand years ago and the y-axis represents the log-scale estimated population size [(Ne*τ), the product of the female effective population size and generation length in years]. The central line represents the median value for the population size, while the shaded area represents the 95% credibility limits. Lineage designations correspond to those in Figure 2.

(2007), our results indicate that *P. forsythii* is not the basal species in the viviparous group. However, these results should be interpreted with caution.

The incongruence across genes is reasonable. It is an inescapable biological reality that gene trees differ for a variety of reasons (reviewed in Maddison, 1997; Degnan and Rosenberg, 2009). Mitochondrial DNA sequence variation in animals is notoriously characterized by a high amount of homoplasy, i. e., genealogical conflict between sites, which decreased the efficiency of mtDNA genes for phylogenetic inference (Engstrom *et al.*, 2004). Historically, it is assumed that the genealogical relationships within a single gene mirrored those that actually occurred in the formation of species. However, it is now widely acknowledged that such direct correspondence between the evolutionary history of genes and of species divergence does not necessarily exist. In cases of rapid speciation, for example, it may actually be more common for gene histories to disagree with one another than to match. Given that conflicting genealogical histories often exist in different genes throughout the genome, it is imperative to take advantage of the direct estimation of species trees, i. e., methods for multilocus species tree inference (Knowles, 2009; Knowles and Kubatko, 2010) to infer a robust phylogeny of the viviparous group of *Phrynocephalus*.

4.2 Taxonomic implications As can be seen from Figure 2, the populations around Qinghai Lake and those from Tianzhu and Guide together form an independently evolving lineage, which seem to be the sister taxon to the rest of viviparous species. In support of several previous studies (Guo and Wang, 2007; Jin, 2008; Nobel *et al.*, 2010; Wang *et al.*, 2002), we recognize that *P. putjatia* is a valid species. In addition, we propose that this species also comprises the populations from North of Qinghai Lake, for example, the populations from Haiyan and Gangcha in this study.

Lineage A1 consisted of the populations from the source region of the Yellow River, including Hongyuan, Xiaman, Maqu and Maduo (Sites 1–7, 22 in Figure 1). This range covers the type locality of *P. vlangalii hongyuanensis*. However, Bedriaga (1909) assigned populations of *P. vlangalii* in the Bailong Jiang region, to *P. v. pylzowi* based on morphological differences. In support of Jin (2008), we agree that *P. v. hongyuanensis* is a synonym of *P. v. pylzowi*.

4.3 Development of divergent lineages within *P.*

***vlangalii* species complex** Our current estimates might not fully reflect the actual diversification time-scales of the *P. vlangalii* species complex because they are based exclusively on mitochondrial data. However, these estimates provide a preliminary timeframe to trace the intraspecific differentiation of the maternal lineages of *P. vlangalii*/*P. putjataia*. Two alternative hypotheses are suggested to explain the development of divergent lineages within a species: the extremely large ancestral population size; or allopatric differentiation in the past (Avise, 2000).

Under the first scenario, we followed Luikart *et al.* (2001) to compute the possible effective size (*Ne*) of an ancestral population necessary to maintain three divergent mtDNA lineages for *P. vlangalii*. To perform this calculation, we assumed the coalescent time of lineages A1, A2 and A3 in the ancestral population to be around 950 000 years ago (Figure 4), or 316 666 generations of 3 years. The expectation of this time is $2Ne\ (1-1/k)$ generations, where k is 105 mt*ND4-tRNA*^{LEU} sequences, implying a *Ne* value of 159 855. The population census size would have to be far larger than this estimated *Ne* (Avise, 2000). It is unlikely that a population of this size was present at any time. Such a large ancestral population is also unlikely for any other toad-headed lizards. Similarly, under the first scenario, we may estimate a *Ne* value of 399 975 for the ancestral population of *P. putjatia*. It is also unlikely that a population of this size was present at any time for *P. putjatia.*

Therefore the second scenario is more likely: namely that the glacial climate drove the lizards into a number of refugia, where the populations diverged. The divergence time of the three lineages of *P. vlangalii* estimated here (*ca.* 0.95 Ma) is roughly consistent with the antepenultimate glaciation events (Kunlun Glaciation) recorded for the QTP during the middle–late Pleistocene (Zheng *et al.*, 2002), which is correlated with MIS l8–l6 (0.78–0.62 Ma). During the most extensive glaciation in the plateau, i. e., Kunlun Glaciation, there were glaciers developing in the Bayun Har and A'nyemaqen Mountains and four big ice caps with a diameter of about 30–50 km. In addition, the subsequent and relatively extensive Zhonglianggan Glaciation occurred between 500 000 and 400 000 years ago (Owen *et al.*, 2006; Shi *et al.*, 1998). Although temperatures rose during the interglacial stages, development of glaciers and/or extremely low temperatures at high elevations (> 4 500 m) throughout the Pleistocene may have continued to impede the gene flow of *P. vlangalii*, eventually resulting in the genetic divergence of *P. vlangalii* in the allopatric regions. In addition, it is worth noting that the A'nyemaqen Mountains appear to have shown significant uplift in the middle Pleistocene during the Kunlun-Huanghe movement (Cui *et al*., 1998), although precise dates are not available. Thus, in support of Jin *et al*. (2008) and Wang *et al.* (2009), we confirm the hypothesis that uplift of the A'nyemaqen Mountains and glaciations since mid-late Pleistocene have promoted the allopartric divergence of *P. vlangalii* in the upper reaches region of the Yellow River.

The Huangshui River valley is situated in eastern Qinghai, China, and between latitude 35°56′–37°38′N and longitude 100°35′–103°05′E. The area belongs to the transition zone between Qinghai-Tibetan Plateau and Loess Plateau with altitudes ranging from 1650 m to 4395 m. The divergence time of the two lineages of *P. putjatia* is estimated as about 1.78 Ma (95% HPD: 0.92–3.06 Ma), which is highly consistent with the final phase of the Qingzang Movement (1.7 Ma; Li *et al.*, 1996). During this phase, there took place accelerated rising at the Xining-Huzhu region, along Huangshui River, the first-class tributary of Yellow River (Lu *et al.*, 2004). There was a significant readjustment of the fluvial catchment during 1.55–1.2 million years ago in the region of paleo-Huangshui, resulting in the modern pattern of Huangshui River. There is no *phrynocephalus* lizards distribution record in the Huangshui River valley and east of Riyue Shan (Zhao, 1997). Tectonic movement in this region was prevalent during this period and is a likely cause of this fragmentation. Subsequently, the glacial climate throughout the Pleistocene may have continued to impede the gene flow of *P. putjatia,* eventually resulting in the genetic divergence of *P. putjatia* in the allopatric regions, e. g., north and southeast of the Qinghai Lake.

Acknowledgements We thank two anonymous reviewers for their valuable comments and suggestions on our manuscript. We are grateful to Dr. Qiang DAI for his assistance in sample collection, and to Dr. Yong HUANG for his help with the artwork. This study was supported by the National Natural Science Foundation of China (30700062), the Knowledge Innovation Program of the Chinese Academy of Sciences (KSCX2-EW-Q-6 and KSCX2-EW-J-22), and the Western Doctor Fund Project of the ''Bright of Western China'' Personnel Training Project.

Appendix

Supplementary material associated with this article can be found in the online version at http://www.ahr-journal.com/.

References

Ababneh F., Jermiin L. S., Ma C., Robinson J. 2006. Matched-pairs tests of homogeneity with applications to homologous nucleotide sequences. Bioinformatics, 22: 1225–1231

Akaike H. 1974. A new look at the statistical model identification. IEEE Trans Automat Contr, 19: 716–723

Aljanabi S. M., Martinez I. 1997. Universal and rapid salt-extraction of high quality genomic DNA for PCR-based techniques. Nucl Acids Res, 25: 4692–4693

Arèvalo E., Davis S. K., Sites Jr J. W. 1994. Mitochondrial DNA sequence divergence and phylogenetic relationships among eight chromosome races of the *Sceloporus grammicus* complex (Phrynosomatidae) in central Mexico. Syst Biol, 43: 387–418

Avise J. C. 2000. Phylogeography: The History and Formation of Species. Cambridge: Harvard University Press, 447 pp

Barabanov A. V., Ananjeva N. B. 2007. Catalogue of the available scientific species-group names for lizards of the genus *Phrynocephalus* Kaup, 1825 (Reptilia, Sauria, Agamidae). Zootaxa, 1399: 1–56

Bedriaga J. V. 1909. Amphibian und reptilien. In Wissenschaftliche Resultate der von NM Prezewalski nach Central-Asien unternomenen Reisen (Zoologischer Theil) St. Petersburg: Band 3 Abt. 1 Annual Reports of the Zoological Museum of Emperor Acad Sci

Brandley M. C., Schmitz A., Reeder T. W. 2005. Partitioned Bayesian analyses, partition choice, and the phylogenetic relationships of scincid lizards. Syst Biol, 54: 373–390

Clement M., Posada D., Crandall K. A. 2000. TCS: A computer program to estimate gene genealogies. Mol Ecol, 9: 1657–1660

Cui Z., Wu Y., Liu G., Ge D., Pang Q., Xu Q. 1998. On Kunlun-Yellow River tectonic movement. Sci Chin Ser D Earth Sci, 41: 592–600

Degnan J. H., Rosenberg N. A. 2009. Gene tree discordance, phylogenetic inference and the multispecies coalescent. Trends Ecol Evol, 24: 332–340

Deng X., Liu S., Ding Y., Shen Y., Zhao L., Xie C. 2004. Quaternary glaciations and environment change in the A'nymaqen Mountains. J Glaciol Geocryol, 26: 305–311 (In Chinese with English abstract)

Drummond A. J., Rambaut A., Shapiro B., Pybus O. G. 2005. Bayesian coalescent inference of past population dynamics from molecular sequences. Mol Biol Evol, 22: 1185–1192

Drummond A. J., Ho, S. Y. W., Pillips M. J., Ranbaut A. 2006. Relaxed phylogenetics and dating with confidence. PLoS Biol, 4: e88

Drummond A. J., Rambaut A. 2007. BEAST: Bayesian evolutionary analysis by sampling trees. BMC Evol Biol, 7: 214

Engstrom T. N., Shaffer H. B., McCord W. P. 2004. Multiple data sets, high homoplasy, and the phylogeny of softshell turtles (Testudines: Trionychidae). Syst Biol, 53: 693–710

Excoffier L., Lischer H. E. L. 2010. Arlequin suite ver 3.5: A new series of programs to perform population genetics analyses under Linux and Windows. Mol Ecol Resour, 10: 564–567

Fan Y., Wu R., Chen M.-H., Kuo L., Lewis P. O. 2011. Choosing among partition models in Bayesian phylogenetics. Mol Biol Evol, 28: 523–532

Felsenstein J. P. 1985. Confidence limits on phylogenies: An approach using the bootstrap. Evolution, 39: 783–791

Fu Y. 1997. Statistical tests of neutrality of mutations against population growth, hitchhiking and background selection. Genetics, 147: 915–925

Gelman A., Rubin D. B. 1992. Inference from iterative simulation using multiple sequences. Stat Sci, 7: 457–511

Guo X., Wang Y. 2007. Partitioned Bayesian analyses, dispersal-vicariance analysis, and the biogeography of Chinese toad-headed lizards (Agamidae: *Phrynocephalus*): A re-evaluation. Mol Phylogenet Evol, 45: 643–662

Harpending H. 1994. Signature of ancient population growth in a low-resolution mitochondrial mismatch distribution. Human Biol, 66: 131–137

Hewitt G. M. 2001. Speciation, hybrid zones and phylogeography–or seeing genes in space and time. Mol Ecol, 10: 537–549

Ho J. W. K., Adams C. E., Lew J. B., Matthews T. J., Ng C. C., Shahabi-Sirjan A., Tan L. H., Zhao Y., Easteal S., Wilson S. R., Jermin L. S. 2006. SeqVis: Visualization of compositional heterogeneity in large alignments of nucleotides. Bioinformatics, 22: 2162–2163

Huelsenbeck J. P., Larget B., Miller R. E., Ronquist F. 2002. Potential applications and pitfalls of Bayesian inference of phylogeny. Syst Biol, 51: 673–688

Jermiin L. S., Ho J. W. K., Lau K. W., Jayaswal V. 2009. SeqVis: A tool for detecting compositional heterogeneity among aligned nucleotide sequences. In Posada D. A. (Ed.), Bioinformatics for DNA Sequence Analysis. Totowa, NJ: Humana Press, 65–91

Jermiin L. S., Jayaswal V., Ababneh F., Robinson J. 2008. Phylogenetic model evaluation. In Keith J. (Ed), Methods in Molecular Biology: Bioinformatics, Vol. I, Data, Sequence Analysis and Evolution. Totowa, NJ: Humana Press, 331–364

Jiang F., Fu J., Wang S., Sun D., Zhao Z. 2007. Formation of the Yellow River, inferred from loess-palaeosol sequence in Mangshan and lacustrine sediments in Sanmen Gorge, China. Quatern Int, 175: 62–70

Jin Y. 2008. Evolutionary studies of *Phrynocephalus* (Agamidae) on Qinghai-Tibetan Plateau. Ph. D. Thesis. Lanzhou University, Lanzhou, 174 pp (In Chinese with English abstract)

Jin Y., Brown R. P., Liu N. 2008**.** Cladogenesis and phylogeography of the lizard *Phrynocephalus vlangalii* (Agamidae) on the Tibetan plateau. Mol Ecol, 17: 1971–1982

Kass R. E., Raftery A. E. 1995. Bayes factors. J Am Statist Assoc, 90: 773–795

Knowles L. L. 2009. Estimating species trees: Methods of phylogenetic analysis when there is incongruence across genes. Syst Biol, 58: 463–467

Knowles L. L., Kubatko L. S. 2010. Estimating Species Trees: Practical and Theoretical Aspects. New Jersey, USA: Wiley-Blackwell Press, 232 pp

Lewis P. O., Holder M. T., Swofford D. L. 2008. Phycas: Software for phylogenetic analysis. Storrs (CT): University of Connecticut. Available from http://www.phycas.org/

Li B., Li J., Cui Z., Zheng B., Zhang Q., Wang F., Zhou S., Shi Z., Jiao K., Kang J. 1991. Quaternary Glacial Distribution Map of Qinghai-Xizang (Tibet) Plateau. Beijing, China: Science Press (In Chinese)

Li J., Fang X., Ma H., Zhu J., Pan B., Chen H. 1996.

Geomorphological and environmental evolution in the upper reaches of the Yellow River during the late Cenozoic. Sci Chin Ser D Earth Sci, 39: 380–390

Li R. 1993. The formation and evolution of Yellow River. In Yang J. (Ed.), Features and Evolution of Landforms in China. Beijing: China Ocean Press

Librado P., Rozas J. 2009. DnaSP v5: Software for comprehensive analysis of DNA polymorphism data. Bioinformatics, 25: 1451–1452

Liu Z., Sun Y. 2007. Uplift of the Qinghai-Tibet Plateau and formation, evolution of the Yellow River. Geogr Geo-Inform Sci, 23: 79–83 (In Chinese with English abstract)

Lu H., Wang X., An Z., Miao X., Zhu R., Ma H., Li Z., Tan H., Wang X. 2004. Geomorphologic evidence of phased uplift of the northeastern Qinghai-Tibet Plateau since 14 million years ago. Sci Chin Ser D Earth Sci, 47: 822–5833

Luikart G., Gielly L., Excoffier L., Vigne J. D., Bouvet J., Taberlet P. 2001. Multiple maternal origins and weak phylogeographic structure in domestic goats. Proc Natl Acad Sci USA, 98: 5927–5932

Macey J. R., Verma A. 1997. Homology in phylogenetic analysis: Alignment of transfer RNA genes and the phylogenetic position of snakes. Mol Phylogenet Evol, 7: 272–279

Maddison W. P. 1997. Gene trees in species trees. Syst Biol, 46: 523–536

Madsen D. B., Ma H., Rhodes D., Brantigham P. J. , Forman S. L. 2008. Age constraints on the late Quaternary evolution of Qinghai Lake, Tibetan Plateau. Quat Res, 69: 316–325

Muelle R. L. 2006. Evolutionary rates, divergence dates, and the performance of mitochondrial genes in Bayesian phylogenetic analysis. Syst Biol, 55: 289–300

Noble D., Qi Y., Fu. J. 2010. Species delineation using Bayesian model-based assignment tests: A case study using Chinese toad-headed agamas (genus *Phrynocephalus*). BMC Evol Biol, 10: 197

Nylander J. A. A. 2008. MrModeltest 2.3. Program distributed by the author. Evolutionary Biology Centre, Uppsala University

Owen L. A., Caffee M. W., Bovard K. R., Finkel R. C., Sharma M. C. 2006. Terrestrial cosmogenic nuclide surface exposure dating of the oldest glacial successions in the Himalayan orogen: Ladakh range, northern India. Geol Soc Am Bull, 118: 383–392

Pan B. 1994. Research upon the geomorphologic evolution of the Guide Basin and the development of the Yellow River. Arid Land Geog, 7: 43–50 (In Chinese with English abstract)

Pang J., Wang Y., Zhong Y., Hoelzel A. R., Papenfuss T. J., Zeng X., Ananjeva N. B., Zhang Y. 2003. A phylogeny of Chinese species in the genus *Phrynocephalus* (Agamidae) inferred from mitochondrial DNA sequences. Mol Phylogenet Evol, 27: 398–409

Posada D., Crandal K. A. 2001. Intraspecific gene genealogies: Trees grafting into networks. Trends Ecol Evol, 16: 37–45

Qu Y., Lei F., Zhang R., Lu X. 2010. Comparative phylogeography of five avian species: Implications for Pleistocene evolutionary history in the Qinghai-Tibetan plateau. Mol Ecol, 19: 338–351

Raftery A. E. 1996. Hypothesis testing and model selection. In Gilks W. R., Spiegelhalter D. J., Richardson S. (Eds.), Markov Chain Monte Carlo in Practice. London, UK: Chapman and Hall, 163–188

Rambaut A., Drummond A. J. 2009. Tracer v. 1.5. Available from http://beast.bio.ed.ac.uk/Tracer

Ramos-Onsins R., Rozas R. 2002. Statistical properties of new neutrality tests against population growth. Mol Biol Evol, 19: 2092–2100

Rogers A. R., Harpending H. C. 1992. Population growth makes waves in the distribution of pairwise genetic differences. Mol Biol Evol, 9: 552–569

Ronquist F., Huelsenbeck J. P. 2003. MrBayes 3: Bayesian phylogenetic inference under mixed models. Bioinformatics, 19: 1572–1574

Shi Y., Li J., Li B. 1998. Uplift and Environmental Changes of Qinghai-Tibetan Plateau in the Late Cenozoic. Guangzhou: Guangdong Science and Technology Press, 463 pp (In Chinese)

Shi Y., Zhao J., Wang J. 2011. New Understanding of Quaternary Glaciations in China. Shanghai: Shanghai Popular Science Press, 213 pp (In Chinese)

Swofford D. L. 2003. PAUP*. Phylogenetic analysis using parsimony (* and other methods), Version 4. Sunderland, MA: Sinauer

Tamura K., Dudley J., Nei M., Kumar S. 2007. MEGA4: Molecular Evolutionary Genetics Analysis (MEGA) software version 4.0. Mol Biol Evol, 24: 1596–1599

Thompson J. D., Gibson T. J., Plewniak F., Jeanmougin F., Higgins D. G. 1997. The CLUSTAL_X windows interface: Flexible strategies for multiple sequence alignment aided by quality analysis tools. Nucl Acids Res, 25: 4876–4882

Wang Y., Zeng X., Fang Z., Wu G., Liu Z., Papenfuss T. J., Macey J. R. 2002. A valid species of the genus *Phrynocephalus*: *P. putjatia* and a discussion on taxonomy of *Phrynocephalus hongyuanensis* (Sauria: Agamidae). Acta Zootaxon Sin, 27: 372–383

Wang Y., Zhan A., Fu J. 2009. Testing historical phylogeographic inferences with contemporary gene flow data: Population genetic structure of the Qinghai toad-headed lizard. J Zool, 278: 149–156

Xie W., Lewis P. O., Fan Y., Kuo L., Chen M. H. 2011. Improving marginal likelihood estimation for Bayesian phylogenetic model selection. Syst Biol, 60: 150–160

Xu T., Abbott R. J., Milne R. I., Mao K., Du F. K., Wu G., Ciren Z., Miehe G., Liu J. 2010. Phylogeography and allopatric divergence of cypress species (*Cupressus* L.) in the Qinghai-Tibetan Plateau and adjacent regions. BMC Evol Biol, 10: 194

Yang S., Dong H., Lei F. 2009. Phylogeogrpahy of regional fauna on the Tibetan Plateau: A review. Prog Nat Sci, 19: 789–799

Yuan B., Chen K., Ye S. 1990. Origin and evolution of Lake Qinghai. Quatern Sci, 3: 233–243 (In Chinese with English abstract)

Zardoya R., Meyer A. 1996. Phylogenetic performance of mitochondrial protein-coding genes in resolving relationships among vertebrates. Mol Biol Evol, 13: 966–942

Zerova G. A., Chkhikvadze V. M. 1984. The review of Cenozoic lizards and snakes of the USSR. Review of Cenozoic lizards and snakes in USSR. Proc Acad Sci Georgian SSR. Series: Biology, 10: 319–325 (In Russian)

Zhan X., Zheng Y., Wei F., Bruford M. W., Jia C. 2011. Molecular evidence for Pleistocene refugia at the eastern edge of the Tibetan Plateau. Mol Ecol, 20: 3014–3026

Zhang Z., Wang S., Yang X., Jiang F., Shen J., Li X. 2004.

Evidence of a geological event and environmental change in the catchment area of the Yellow River at 0.15 Ma. Quatern Int, 117: 3–40

Zhao J., Shi Y., Wang J. 2011. Comparison between Quaternary Glaciations in China and the marine oxygen isotope stage (MIS): An improved schema. Acta Geogr Sin, 66: 867–884 (In Chinese with English abstract)

Zhao K. 1997. Notes on the Chinese toad-headed agamids and its diagnostic characters. J Suzhou Railway Teachers Coll, 14: 27–32

Zhao K. 1999. *Phrynocephalus* Kaup, 1825. In Zhao E., Zhao K., Zhou K. (Eds.), Fauna Sinica Reptilia, Vol. 2. Beijing: Science Press, 153–193 (In Chinese)

Zheng B., Rutter N. 1998. On the problem of Quaternary glaciations, and the extent and patterns of Pleistocene ice cover in the Qinghai-Xizang (Tibet) Plateau. Quatern Int, 45/46: 109–122

Zheng B., Wang S. 1996. A study on the Paleo-glaciation and paleoenvironment in the source area of the Yellow River. J Glaciol Geocryol, 18: 210–218 (In Chinese with English abstract)

Zheng B., Xu Q., Shen Y. 2002. The relationship between climate change and Quaternary glacial cycles on the Qinghai-Tibetan Plateau: Review and speculation. Quatern Int, 97/98: 93–101

Zhou S., Li J., Zhao J., Wang J., Zheng J. 2011.Quaternary Glaciations: Extent and Chronology in China. In Ehlers J., Gibbard P. L., Hughes P. D. (Eds), Developments in Quaternary Science, Vol. 15, Amsterdam, The Netherlands: Elsevier Press, 981–1002

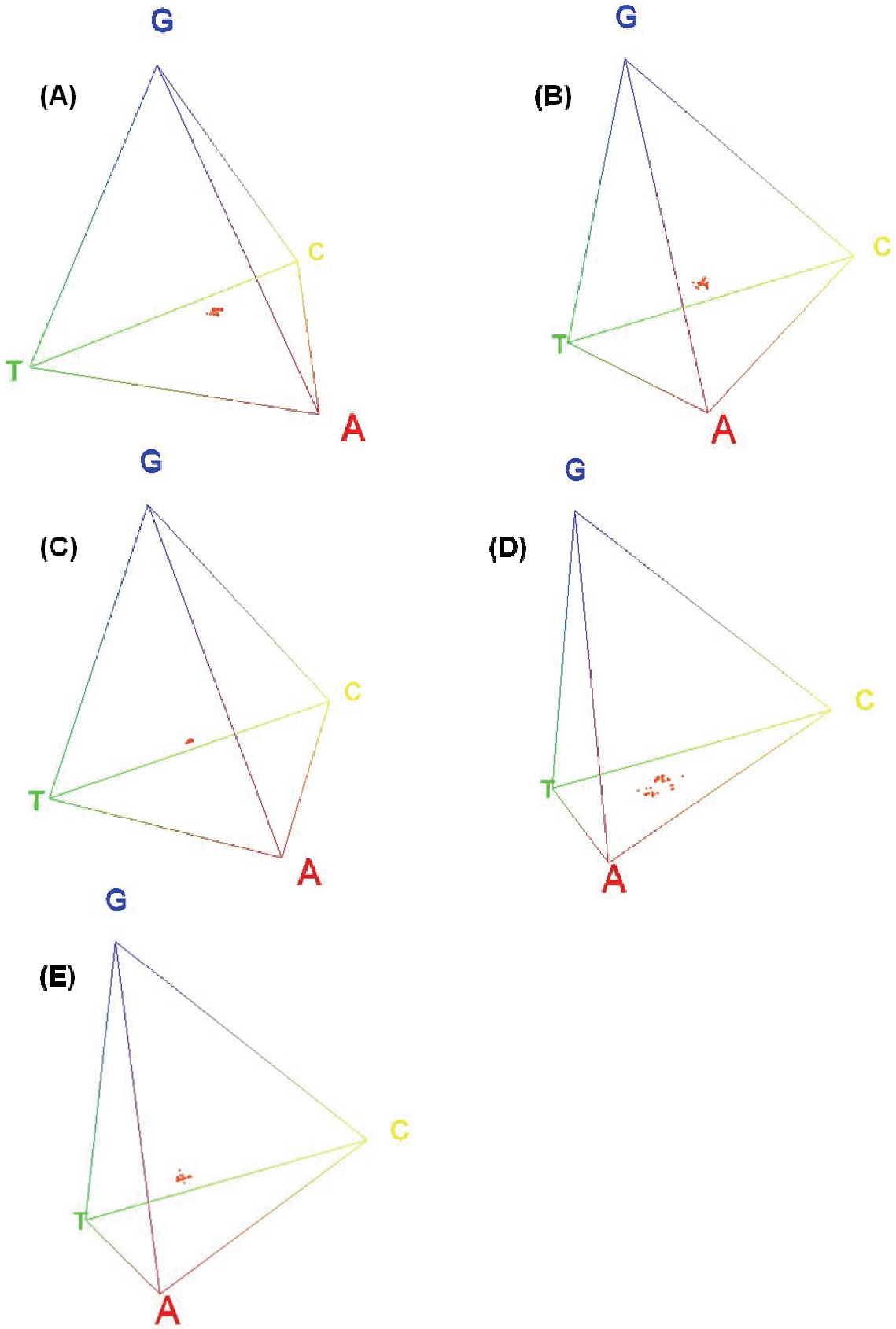

Appendix 1 Tetrahedral plots. (A): all sites of *ND4-tRNA*^{LEU}; (B): first codon sites; (C): second codon sites; (D): third codon sites; and (E): tRNAs sites. The plots were obtained using the *Choice of Sites* command from the View menu in the program SeqVis v.1.5 (Ho *et al.*, 2006).

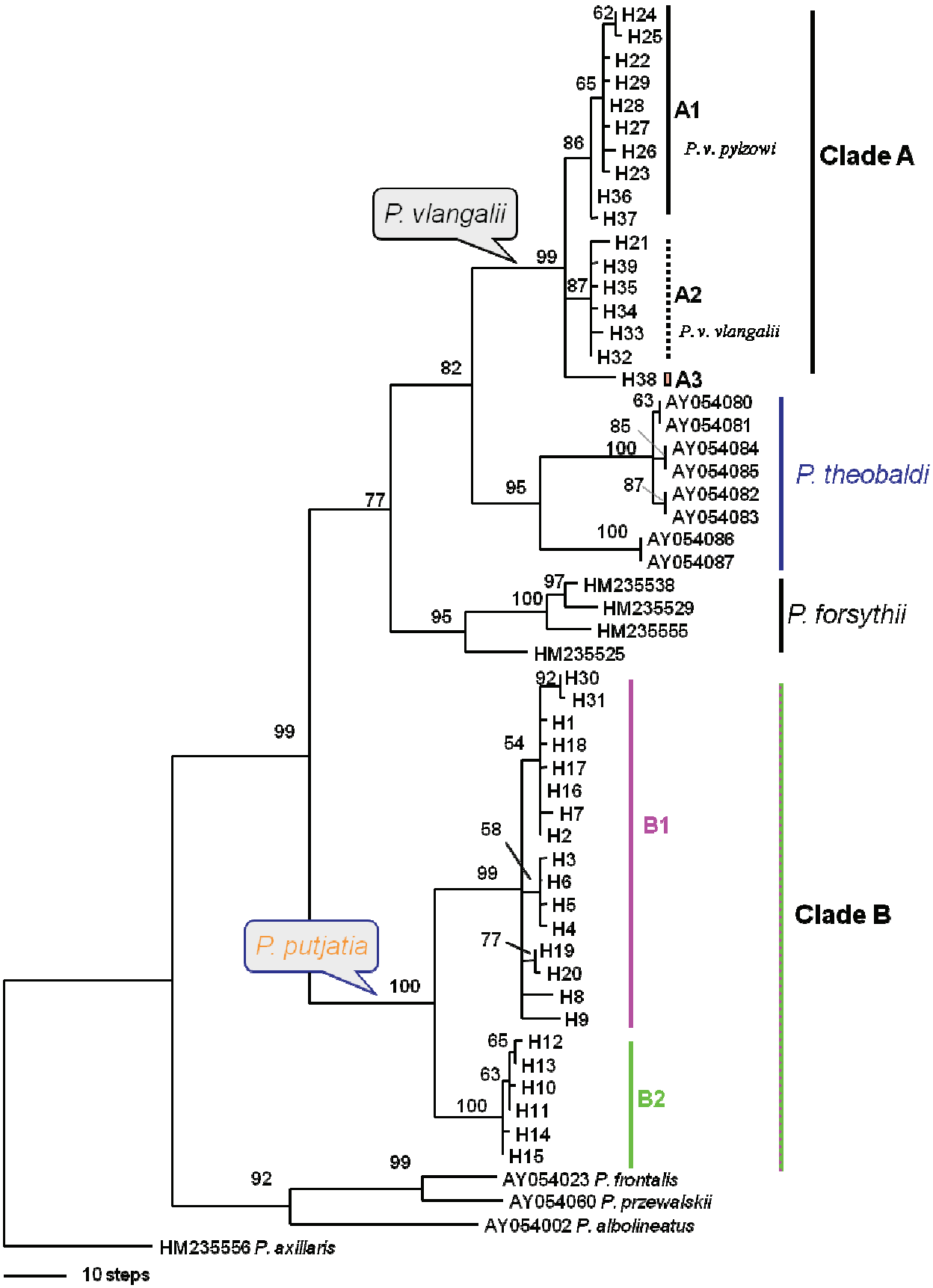

Appendix 2 Maximum parsimony consensus tree from 1 000 bootstrap replicates of *ND4-tRNA*^{LEU} by using PAUP*, with gaps treated as missing data. Numbers above the branch represent percent recovery in bootstrap analysis (1 000 pseudoreplicates). Tree length = 423, CI = 0.5816, RI = 0.9052.